A novel pressure array sensor based on contact resistance variation: Metrological properties

Z. Del Prete, L. Monteleone, and R. Steindler

Citation: Rev. Sci. Instrum. **72**, 1548 (2001); doi: 10.1063/1.1340561
View online: http://dx.doi.org/10.1063/1.1340561
View Table of Contents: http://rsi.aip.org/resource/1/RSINAK/v72/i2
Published by the American Institute of Physics.

A novel pressure array sensor based on contact resistance variation: Metrological properties

Z. Del Prete, L. Monteleone,[a] and R. Steindler
Department of Mechanics and Aeronautics, University of Rome ''La Sapienza,'' Via Eudossiana 18, 00184 Roma, Italy

(Received 2 August 2000; accepted for publication 20 November 2000)

The working principle and the metrological performances of a novel array sensor devoted to pressure map measurements are experimentally analyzed here. The physical principle on which the sensor elements are sensitive to the pressure is the variation of the contact resistance. Pressure maps from 1 up to 500 kPa can be measured. The prototype here utilized for the metrological characterization has been an 8×8 matrix sensor with a 5 mm spatial resolution over both x and y direction and a total thickness of 150 μm. The materials that have been chosen to assemble the prototype yielded to a very flexible and robust sensor which can easily be fitted over round surfaces without being damaged or leading to an alteration of its measuring properties. The static and the dynamic metrological performances of the sensor that have been studied and discussed are the response function and the calibration curve, the repeatability, the sensitivity, the time drift, the hysteresis, and the dynamic response. In spite of its functional and constructive simplicity, the metrological performances the sensor has exhibited, together with its peculiar constructive feature, have indicated the possibility to utilize it to effectively measure pressure maps in every application for which the sensor could be shaped in. © *2001 American Institute of Physics.* [DOI: 10.1063/1.1340561]

I. INTRODUCTION

The study of pressure maps is a subject matter of great importance in many different fields as scientific measurement, biomedical research, and industrial application. In robotics, for example, it is very useful to know the force applied by the pliers to assure a correct manipulation of objects or, there where artificial tactile organs are required, for the recognition and the distinction of shapes. In ergonomics the primary interest is to measure the pressure distribution and the overall force that is required to hold, for example, the handle of a tool or, may be, a doorknob. On the other side, during the rehabilitation practice involving functional electrical stimulation to obtain a partial grip restoration for quadriplegic patients, the knowledge of the force produced by the fingers under electrical stimulation allows to dimension in the correct way the feedback system of the grasp itself, also with the aim to avoid unnecessary fatigue to the patient. Other medical applications used for diagnosis are the force measurement exerted during byte done by dentists and the measurement of foot pressure during the walk in gait analysis done by orthopedist.

Several different types of sensors have already been proposed for the aforesaid applications.[1–9] These proposals comprise many capacitive sensors, few optical sensors, piezoelectric, and piezoresistive sensors. The ones based on capacitance variation have been proposed in many different shapes and also in a matrix configuration. These sensors exhibit a spatial two-dimensional (2D) resolution up to 1 mm^2. They are sensitive also to shear load, have the advantage of being simple, and can easily be realized. On the other hand, the capacitive sensors have the major drawback and their utilization is generally limited to dynamic applications. Optical sensors, which have been proposed primarily for gait analysis, do not perform a great spatial sensitivity and are encumbering as regards the overall dimensions and, most importantly, the thickness. Piezoelectric sensors are generally made of PVDF film elements and, therefore they are very thin. These kind of sensors are unable to keep track of static loads and are utilized basically as on-off sensors.

The piezoresistive sensors are the ones that result quite similar to the one proposed here: in fact, while the piezoresistive ones show a change in the material resistance with the applied pressure, the proposed sensor is characterized meanly by the contact resistance variation (see further). The sensor here proposed is a surface array transducer with the active elements arranged within a sandwich structure. It has several advantages in respect to other commercial realizations: it is of very simple design and made with low-cost materials easily found on the market; it is a resistance variation sensor, therefore it can be supplied with a direct current which allows the utilization for static applications. The $m\times n$ matrix design allows to reduce the electrical connections to the active elements from $2(m\times n)$ down to $m+n$.

Piezoresistive sensors are already available on the market and are also shaped in matrices. They are generally sold only in conjunction with the compatible acquisition unit. The piezoresistive sensing elements are made either of solid materials and, sometimes, fluid or gel drops.[10] These are generally patented materials and it has not been possible to find in the literature clear and complete information about their metrological performances.

[a]Electronic mail: monteleo@dma.ing.uniroma1.it

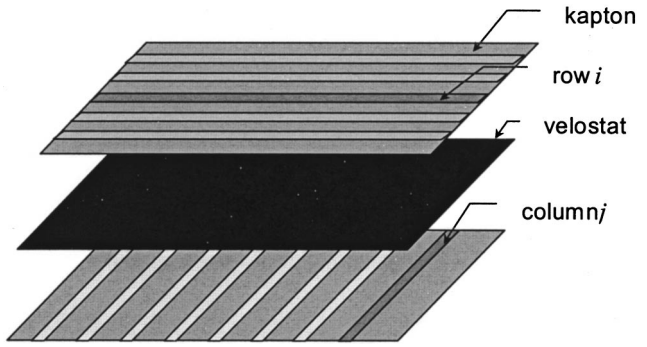

FIG. 1. The sensor has a sandwich structure: the two external sheets, where the conductive rows and columns are electroplated, are made of a plastic material (kapton) and a resistive polymer sheet (velostat) is inserted between them. The crossing of the row i with the column j is the pressure active element of the sensor.

Thus, the aim of the present research has been the description of a novel contact resistance matrix sensor and its working principle but, more important, the experimental analysis of its metrological properties both for static and dynamic measurement conditions.

The pressure measurement range and the calibration curve have been obtained together with the sensitivity threshold; the repeatability, the hysteresis, the time drift and the rapidity of the proposed sensor have been studied.

The knowledge of the proposed sensor's metrological properties allows the experimentalist to utilize such kind of sensor with the awareness of its advantages but also of its limitations.

II. SENSOR SETUP AND EXPERIMENTAL FACILITIES

The proposed contact resistance pressure array sensor has a simple and peculiar sandwich structure. As shown in Fig. 1, the two external sheets which are 40 μm thick are made of a plastic material (Kapton). The conductive rows and columns of the matrix are electroplated on the internal side of the Kapton sheets. A resistive polymer sheet (Velostat) with a thickness of 70 μm and a specific resistance of 11 kΩ/cm^2, is inserted between the two Kapton sheets. The sensor overall thickness results therefore around 150 μm. The rows and the columns of the matrix are formed assembling the two external Kapton sheets with the conductive lines facing the Velostat and each other orthogonal (see Fig. 1). The crossing of row i with column j originates the active element sensitive to pressure. The prototype here analyzed had the electroplated conductive lines 2.5 mm wide, distant each other 2.5 mm, therefore the pitch, which is actually the spatial resolution, was 5 mm and the active area, which is a single active element, resulted 25 mm^2.

The physical principle for which the sensor active elements are functioning has been identified in the variation of the contact resistance between the Velostat and the couple of orthogonal conductive lines electroplated on the Kapton when a pressure is exerted on the underlying 25 mm^2 area. Some preliminary tests have shown the negligible contribution of the Velostat sheet to the whole resistance variation.

A scheme of the working principle is reported in Fig. 2. When no pressure is applied to the sensor, there is only a

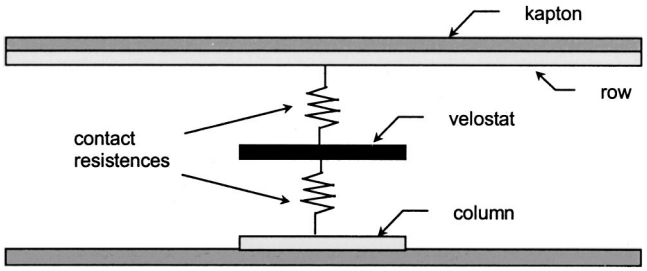

FIG. 2. The working principle of the sensor element is the contact resistance variation between the resistive polymer and the conductive rows and columns when a pressure is applied to the element.

casual and negligible contact between the conductive lines and the resistive polymer: the active elements behave as an open circuit and exhibit an infinite resistance. When a pressure is applied, the contact area at a microscopic level between the electroplated lines and the polymer underlying area increases proportionally to the external load and the correspondent electrical resistance decreases. The measurement of the electrical resistance existing between each crossing of the conductive rows and columns leads to the measure of the applied pressure map.[11]

The sensor has a matrix structure and, to obtain the correct pressure map, it requires the correct readout for each active element. The readout query can be done in two different ways:

(1) one by one for each active element, by means of a direct measurement of the electrical resistance existing at the crossing of row i and column j while electrically disconnecting each other element; and
(2) sequentially for each matrix node (active area or element) utilizing a scanning circuitry.

The first kind of query has been adopted only for the calibration and the repeatability tests whereas the second has been utilized for every other test and application.

The electronic circuit, which has been utilized to simultaneously scan the matrix elements, is a modification of the Purbrick circuit.[12] The electronic scheme of the scanning circuit for a 3×3 sensing array is reported in Fig. 3. Compared to the original Purbrick circuit we add a second multiplexer for the columns which allows to apply at the nonselected rows, the voltage measured at the selected one and, thus, compensates for intrarow eddy current.

The sensor which has been utilized for the metrological characterization was an 8 row$\times$8 columns. In this realization, as shown in Fig. 4, the Velostat resistive polymer has been cut in stripes which have been laid exactly under the electroplated conductive lines identified in the system as the columns. That has been done to realize a physical isolation between columns and, therefore, to inhibit the intracolumn eddy currents which the scanning circuit was not able to compensate for.[13]

The data coming out from the whole array sensor have been scanned by the electronic device just mentioned and digitized with an automatic acquisition system. This unit was a 12 bit analog-to-digital converter with a maximum sampling frequency of 100 kHz properly synchronized with the

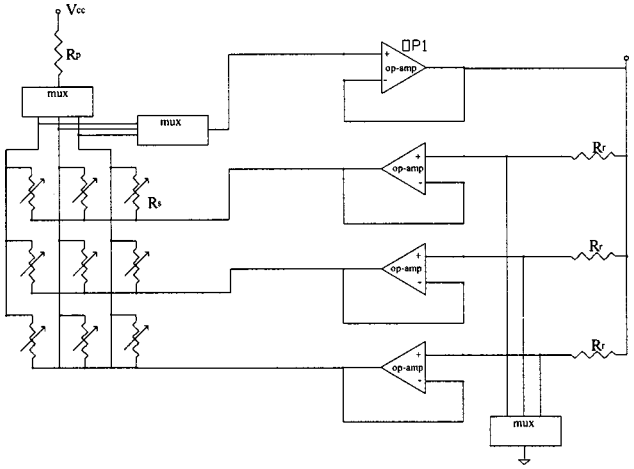

FIG. 3. The scheme of the modified Purbrick circuit, here simplified for a 3×3 sensing array, used for the simultaneous scanning of the matrix elements.

electronic scanning device. Digitized data were dumped on a standard PC Pentium II–350 MHz where they were analyzed and plotted in real time on the monitor as a 2D color map.

A mechanical experimental setup has been designed and realized to test the array sensor. The lateral view of the apparatus is reported in Fig. 5. The setup makes it possible to apply known and established trend loads. The test apparatus consisted of a frame, an operating head, and a sensor bearing plate which could provide for *xy* movements. The frame structure is the same of a drilling machine so, vertical movements of the operating head were also possible. The operating head consisted of a load cell with a 0–100 N range and a 100 mV/N sensitivity, of a voltage driven shaker (B&K 4810), and of some interchangeable loading front ends with well-known finished final surfaces.

III. SENSOR METROLOGICAL PROPERTIES

A. Calibration

The measuring range and the calibration curve have been carried out applying known pressures to one single array element. The 5.5 mm diameter front end of the apparatus has been pushed to the active element with gradually increasing forces. To this aim, the force actuator (shaker) has been gradually driven with 0.2 N force steps, which correspond to

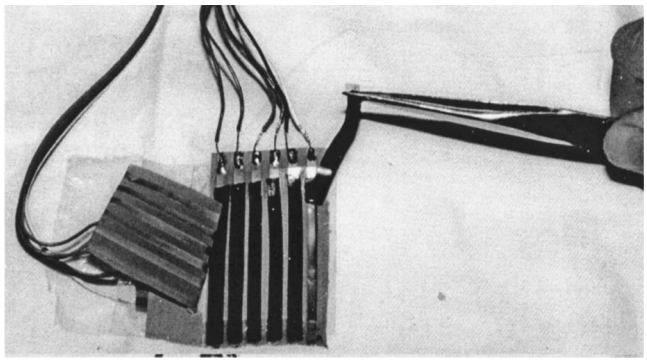

FIG. 4. The final design of the sensor: the resistive polymer has been cut in strips and adapted on the conductive lines identified as columns.

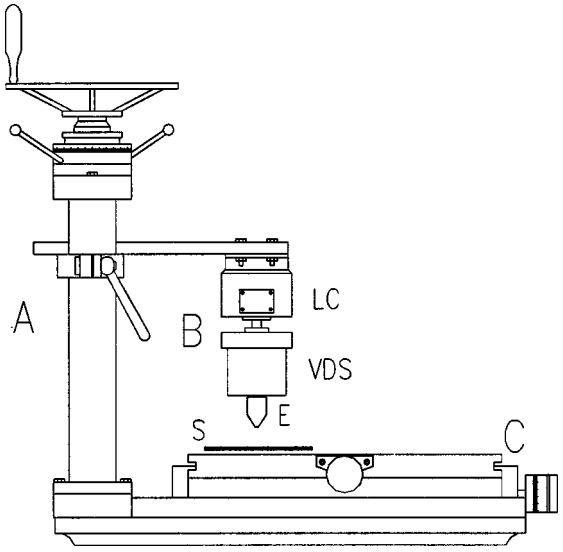

FIG. 5. The lateral view of the mechanical set up used to test the sensor (A: the frame; B: the operating head; C: the sensor bearing plate; LC: the load cell; VDS: the voltage driven shaker; E: the front end; and S: the sensor).

8.4 kPa pressure steps applied to the sensor. The steps have been applied allowing each time for a few seconds rest before applying the next pressure step, so a discontinuous step sequence has been chosen for the trial.

The sensor active element output has been measured one second after load application. The sensor resistance and the load cell output have been easily measured with two multimeters.

With the earlier mentioned modality, for each element of the array sensor a mean calibration curve $R_i(p)$ has been calculated with the following formula:

$$R_i(p)=\frac{\Sigma_{j=1}^{N} r_{ij}(p)}{N}, \tag{1}$$

where j=number of times the calibrations have been repeated and $r_{ij}(p)$=calibration curve j for the active element i.

In this research we limited the number of times the calibration curves have been repeated for each node to three.

The sensor calibration curve which can be considered valid for all the active elements $R(p)$ has been calculated starting from each element calibration curve $R_i(p)$ with the following equation:

$$R(p)=\frac{\Sigma_{i=1}^{m\times n} R_i(p)}{m\times n}, \tag{2}$$

where m=columns, n=rows, and $m=n=8$ (as said before).

$R(p)$ is the mean calibration curve available for the whole sensor and is representative of the mean response of each sensor element within the measurement range; it has been applied to every active element of the array sensor under the hypothesis that each element would respond the same way following the calculated calibration function. The limits of such a hypothesis are quantified and discussed for our sensor in the next paragraph where the results of the measurement repeatability passing from active element to active element are reported.

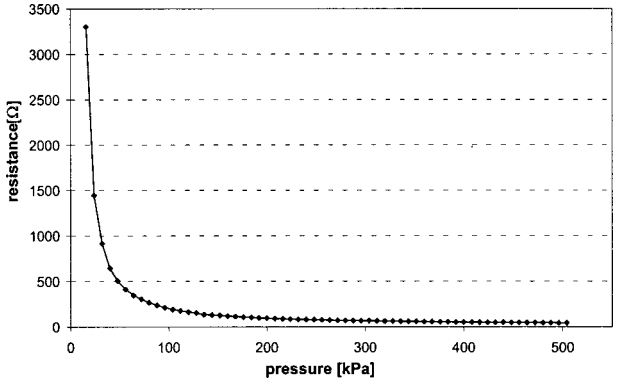

FIG. 6. The resistance response of the sensor as a function of the applied pressure resulting from the global calibration curve $R(p)$.

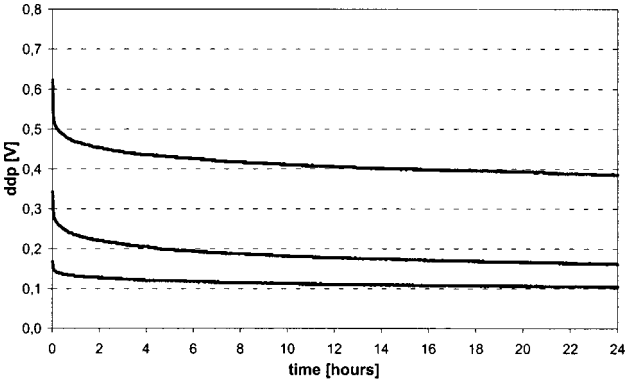

FIG. 7. The drift trend of the sensor during 24 h for different loads: 50 kPa (upper trace), 100 kPa (middle trace), and 200 kPa (lower trace).

The global calibration curve $R(p)$ calculated for our sensor is shown in Fig. 6. The sensor is far from being linear and has a very steep initial part; then it shows an hyperbolic trend up to a pressure value around 500 kPa, after which the curve adjusts over an asymptotic resistance value (19 Ω) for which the sensor full scale appears to have been reached. This value represents also the maximum pressure the sensor active elements are able to measure; indeed trying to load the sensor with higher pressures than this value did not result in any further resistance variation, indicating that a saturation condition had been reached as regards the contact between the electrodes and the interposed resistive polymer.

From the experimental curve $R(p)$ a least squared error best fitting has been calculated, which provided an interpolated curve subdivided in two stretches: the first one from 0 to 16 kPa results linear while the second one is hyperbolic as reported hereafter

$$\begin{cases} R = -7300p - 1584, & \text{for } p \leqslant 16 \text{ kPa}, \\ R = \dfrac{51.93}{p^{1.47}} + 19, & \text{for } p > 16 \text{ kPa}. \end{cases} \tag{3}$$

Resistance R values are expressed in ohms.

B. Repeatability

It has been hypothesized earlier that every active element of the matrix would follow the same calibration curve $R(p)$ calculated with Eq. (3) but, being the sensor made of many different active areas, which lead to a sampled sensitive surface, it is still necessary to provide for the measurement repeatability from one active element to another and to evaluate their deviations from the mean calibration curve $R(p)$.

For each active element the deviation of $r_{ij}(p)$ from the element mean calibration curve $R_i(p)$, which accounts for the time repeatability of a single active element has been first tested. Afterwards the deviation of the $R_i(p)$ curves from the overall calibration curve $R(p)$ which account for the spatial repeatability among different active elements has also been calculated. The deviations of the three $r_{ij}(p)$ from the respective $R_i(p)$ curves indicated an overall error within 15% of the measured values for pressures up to 50 kPa and lower than 5% for pressures from 50 kPa to the saturation point. The measurement repeatability of the single active array elements has therefore been considered quite satisfactory.

As concerns the deviation of the individual calibration curves $R_i(p)$ from the overall curve $R(p)$, the results showed deviations between 20% and 30% for pressures below 150 kPa and between 10% and 20% for higher pressures, up to the saturation point. These deviations appear of some weight, especially for those situations in which the pressure load is applied on a low number of elements (<10). However, for wide pressure maps, when the load is spread over a higher number of elements, although with the limitations set by the measured deviations, the application of one single overall calibration curve for the whole sensor appears still justified.

C. Time drift

As already explained, the core material laid between the electrodes which is mainly responsible for a correct pressure transduction is the Velostat resistive polymer. Even if the polymer is utilized here as a thin sheet (70 μm) it undergoes a mechanical strain when loaded and stressed along its surfaces. Strain behavior influences the contact between the polymer itself and the electrodes and, therefore, introduces time drift. The issue is there maybe a better contact between the polymer and the electrodes which develops with time and causes a further resistance decrease.

The drift tests have been carried out both for short and long term to study the sensor's time drift behavior. Constant pressure values of 50, 100, and 200 kPa have been applied to the active elements for time intervals of 15 min, 30 min, and 24 h. The results obtained for one active area located in the center of the sensor are shown in Fig. 7. Other active elements exhibited analogous results.

For smaller loads the drift results initially steeper and evolves faster in time, whereas for higher loads the drift is not so steeper at the beginning and has a flatter tendency; in the first 50 s for a 50 kPa load the drift reaches 17% while for 100 kPa and for 200 kPa it results 12% and 10%. In the 24 h interval the observed drifts were as follows: 44% for a 50 kPa load, 36% for 100 kPa, and 33% for 200 kPa. It seems important to outline that for the last 4 h the drift could be considered negligible since only 2%, 1%, and 0.75% have been observed respectively for 50, 100, and 200 kPa load.

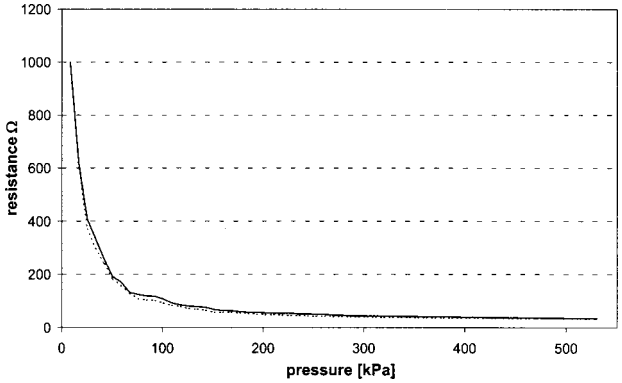

FIG. 8. The sensor output during a load (continuous line) and unload (dotted line) cycle. The maximum hysteresis takes place at a pressure around 50 kPa.

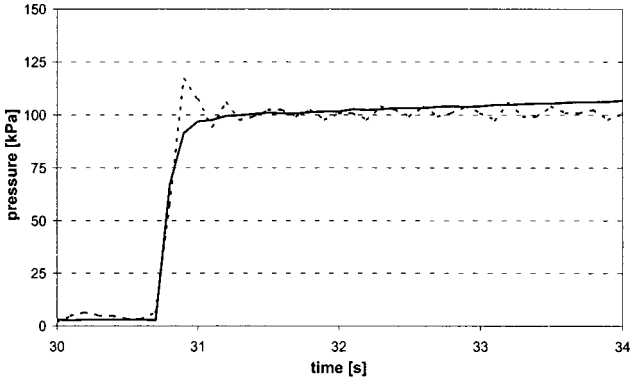

FIG. 9. The sensor output (continuous line) during a step load (dotted line) test; no delay has been observed between the load and the sensor output.

During the experiments done to test the sensor dynamic properties, which are reported in detail in the next paragraph, the sensor output has been acquired for short periods; with high sampling rate, we observed that the sensor active elements start to drift from their initial stabilized output value not immediately but 2 s after the load had been applied. This observation justifies the choice of considering as the true output value during the calibration process the output measured after 1 s the load had been applied.

At the present stage of the sensor development the observed drifts certainly limit the sensor utilization for long term applications when the measurements have to go on for hours or, may be for days; nonetheless the vast majority of the application the sensor has been developed for (as gait analysis), are definitely dynamic with a main frequency $f > 1$ Hz. Moreover, what previously said about no literature references regarding the properties of other similar sensors can be repeated particularly with regard to the sensor drift.

D. Hysteresis

To carry out hysteresis tests the sensor active elements have been cyclically loaded up to their full scale pressure value and then discharged to zero.

The results of this test are reported in Fig. 8. The highest hysteresis value, which has been calculated as one half of the percent deviation between loading and unloading values resulted equal to 7% at a pressure around 50 kPa. On the flat tract of the curve for pressures bigger than 100 kPa hysteresis resulted much lower. From the results it can be stated that the hysteresis does not influence negatively the sensor output.

E. Dynamic response

The dynamic tests have been performed applying a pressure step to some sensor active elements and measuring the element output delay. Pressure steps have been applied through the dynamic actuator DV of Fig. 5 which loaded the sensor active area with a 0.6 N force square wave. The transient observed for a positive step both for the load cell and the sensor was about 10 ms: no response delay was observed between actuator and sensor as reported in Fig. 9. The same result has been observed for a negative pressure step, when the sensor active elements were unloaded. No differences in the dynamic behavior have been noted between the central and the border active elements.

Considering the sensor negligible mass and the imperceptible displacements involved in the pressure measurement and that no capacitive or inductive electrical parameter have a significant role in the sensor measurement process, from the previous results this contact resistance pressure sensor can be considered a zero order system[14] and for the frequencies involved in typical mechanical applications (<10 kHz) the sensor elements respond almost instantly.

The main dynamic limitations are therefore to be searched in the scanning and acquisition system speed in relation with the active elements number.

F. Sensitivity threshold

When a pressure distribution has to be reconstructed by means of a map, it is important to determine which areas of the array sensor are of primary interest, especially when many elements are activated to measure pressure maps distributed over a wide surface. Such a necessity leads to study the activation threshold of the array elements, which here is intended that pressure value for which the contact resistance changes start to be regular.

To carry out the threshold tests the sensor has been loaded with a 380 mm^2 head, applying a 10 mHz triangular variable force wave with a maximum amplitude of 5.8 N. That load corresponded to a maximum pressure of 15 kPa on four active elements simultaneously.

During the loading ramp of the triangular wave a point has been observed for which the sensor elements start signaling the pressure. For this points the pressure measured from the sensor elements has been compared to the load applied with the actuator and measured with the load cell LC of Fig. 5.

The results of the threshold tests relative to four active elements are reported in Fig. 10. The mean threshold value calculated for all the active areas resulted equal to 1 ± 0.2 kPa. Therefore, each element which, during the sensor utilization, indicated a pressure value lower than the threshold one had been zeroed and the corresponding elements had been considered not activated.

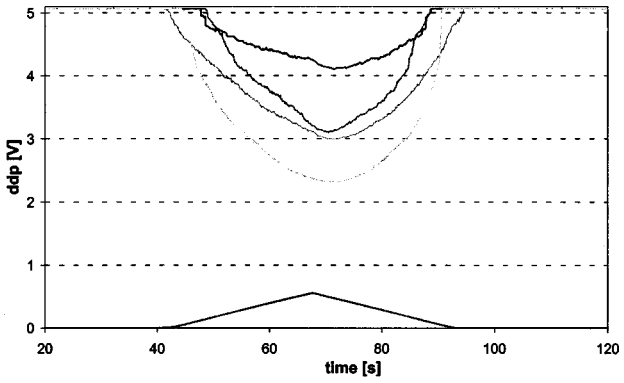

FIG. 10. The response of four elements of the matrix (upper traces) for a triangular load (lower trace) during the threshold test. The maximum pressure simultaneously applied on four elements is 15 kPa.

IV. DISCUSSION

The array sensor exhibited good performances for some of the analyzed properties: it showed a low threshold level which could allow to measure incipient pressures in those applications as the nonslipping condition measurement in hand grip. Nevertheless, other metrological properties resulted of a lower level: the response homogeneity between the single active elements should be improved to allow the utilization of a single calibration curve for every active area of the sensor with a better accuracy. Long term drift resulted the property with the lowest quality. Differently from the accuracy this flaw might not easily be corrected because it depends on the particular elasticity of the resistive polymer, which, on the other hand, is a necessary feature to obtain a flexible sheet sensor applicable on curved surfaces. Moreover, the authors were not able to find on the market or even in the literature, a sheet pressure map sensor with no long term significant drift.

[1] P. Crago, J. Chizeck, M. Neuman, and T. Hambrecht, IEEE Trans. Biomed. Eng. **33**, 256 (1986).
[2] T. D'Alessio and R. Steindler, Med. Eng. Phys. **17**, 466 (1995).
[3] J. G. Webster, *Tactile Sensors for Robotics and Medicine* (Wiley-Interscience, New York, 1988).
[4] J. Volf, S. Holy, and J. Vlcek, Sens. Actuators A **62**, 556 (1997).
[5] S. Son Jae, M. R. Cutosky, and R. D. Howe, Rob. Auton. Syst. **17**, 217 (1996).
[6] M. Arcan and D. Prutchi, Measurement **11**, 197 (1993).
[7] D. J. Beebe, D. D. Denton, R. Radwin, and J. G. Webster, IEEE Trans. Biomed. Eng. **45**, 151 (1998).
[8] T. H. Speeter, Int. J. Robot. Res. **9**, 25 (1990).
[9] R. S. Fearing, Int. J. Robot. Res. **9**, 3 (1990).
[10] J. K. Otto, T. D. Brown, and J. J. Callaghan, Exp. Mech. **39**, 317 (1999).
[11] T. Tamai, IEEE Trans. Compon., Hybrids, Manuf. Technol. **5**, 56 (1982).
[12] J. A. Purbrik, Proceedings of the 1st International ROVISEC Conference, 1981, pp. 73–80.
[13] L. Monteleone and R. Steindler 9th Conference for Sensors Transducers and Systems, 1999, pp. 299–304.
[14] T. G. Beckwith, *Mechanical Measurements* (Addison-Wesley, New York, 1993).